

# Hydrogen-Sensing Characteristics of Palladium-Doped Zinc-Oxide Nanostructures

*Undergraduate Researcher*  
Saranya Sathanathan  
University of Tennessee, Knoxville

*Faculty Mentor*  
Vinayak P. Dravid  
Department of Materials Science and Engineering  
Northwestern University

*Graduate Student Mentor*  
Shan-Wei Fan  
Department of Materials Science and Engineering  
Northwestern University

## Abstract

Semiconductor oxides are important materials in gas-detection systems and can be improved by enhancing the sensitivity and selectivity of oxide sensors to specific gases. This research investigates the effect of palladium dopant (Pd) on the hydrogen gas-sensing ability of ZnO 2-D nanostructures. Photolithography was used to pattern electrodes on various concentrations of Pd-doped ZnO thin films deposited on silicon oxide substrate, and these devices were subsequently used to measure the electrical resistance in response to hydrogen gas flow. Both nanostructure characterization and gas-sensing characterization were conducted on the ZnO thin-film samples. For the nanostructure characterization of the thin films, scanning electron microscopy (SEM) was used to determine the effect of various concentrations of dopant on the grain structure. Energy dispersive spectrometry (EDS) and x-ray photoelectron spectroscopy (XPS) were used to verify the composition of the Pd-doped ZnO thin films, and inductively coupled plasma (ICP) was used to determine the concentration of the doped sol gels. X-ray diffraction (XRD) was used to determine the crystal structure of the doped thin films. For the gas-sensing characterization, the three key assessments used to characterize the sensitivity of ZnO thin films were comparisons between ZnO thin-film sensors and a commercial sensor, comparisons between 2-D ZnO thin-film sensors and 1-D nanolines, and the exposure of the ZnO thin films to UV light.

## Introduction

A gas sensor is a device that is used to detect the presence or amount of a particular gas. Metal oxides have been undergoing extensive research due to their gas-sensing capabilities and have been applied in the automotive and aerospace industries for the detection of exhaust gases for environmental protection; the domestic sector in fire alarms and carbon monoxide sensors; the medical field for patient monitoring and diagnostics; and security and defense departments for tracing explosives and toxic gases.<sup>1</sup>

One of the most critical needs in gas sensing is to develop hydrogen sensors for detection in biological functions and in fuel cells that are able to selectively detect hydrogen gas near room temperature and that are relatively inexpensive and portable.<sup>2,3</sup> Zinc oxide, an oxide semiconductor, is an important prospect for hydrogen gas sensing because it is biosafe and its nanostructures are simple to fabricate. Four main factors that affect its hydrogen-sensing ability still need to be studied and optimized: sensitivity, selectivity, stability, and response and recovery time.<sup>2,4</sup>

Sensitivity — the ability to detect minute quantities of a gas — affects the performance of a gas sensor.<sup>5</sup> A large surface-to-volume ratio corresponds to a higher sensitivity, which has led to an interest in oxide nanostructures, which have ultrahigh surface-to-volume ratio.<sup>1</sup> Another very important property of a gas sensor is selectivity — being able to distinguish a particular gas from all others. Oxides cannot easily distinguish between different types of gases, but adding certain dopants to them increases their selectivity. Another problem with oxide sensors is that they require high operating temperatures, which degrade the material and reduce the stability of the nanostructure sensors. The response and recovery time, or the time taken for the sensor to reach 90% of its saturation after applying or switching off the particular gas, is another important factor in the performance of a gas sensor.<sup>5</sup>

The primary goal of this research is to study the effect of varying the concentration of Pd dopant in ZnO 2-D thin-film nanostructure devices in order to optimize the devices' performance during exposure to hydrogen gas.

## Background

Gas-sensor devices operate by converting chemical information from a chemical reaction with the gas molecule to an analytical signal.<sup>5</sup> Zinc oxide gas-sensor mechanisms involve the adsorption of oxygen on the

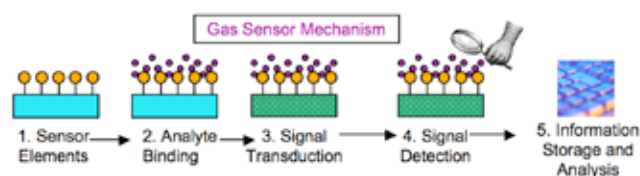


**Figure 1.** The gas-sensing mechanism can be explained by five processes. (1) Sensor elements consist of the different type of structures of the gas-sensing material. (2) Analyte binding involves the binding of target gas molecules onto the surface of the sensor elements. (3) Signal transduction involves a surface reaction occurring between the target gas molecules and the surface of the sensor elements, which consists primarily of oxidation-reduction reactions between the oxygen on the surface and the target gas molecule. (4) The chemical reaction on the surface is interpreted by a change in resistance of the gas-sensor device. (5) The observed change in resistance is then recorded and analyzed.

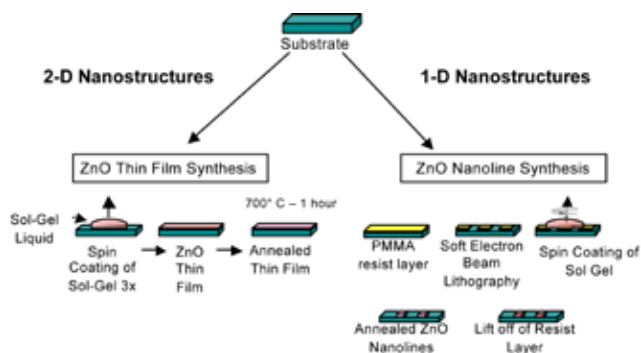


**Figure 2.** The ZnO thin films were fabricated by spin-coating ZnO sol gel on the surface of silicon oxide wafer three times and then annealing the films at 700° C to crystallize the ZnO. The ZnO nanolines were fabricated using soft-electron beam lithography in which an electron beam resist is spin-coated on top of the substrate, and a high-energy electron beam is used to pattern the top of the substrate. The exposed regions of the resist are removed, which then allows the sol gel to be spin-coated on top of the substrate. Lift-off occurs where the photoresist is removed, leaving only the ZnO nanopattern on top of the substrate. The nanopattern is then annealed.

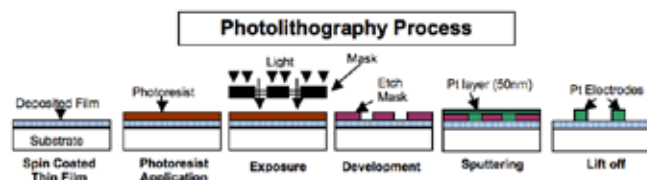


**Figure 3.** The photolithography process was used to create Pt electrodes on top of the ZnO thin film in order to conduct the electrical property measurements of the ZnO thin films.

oxide surface and create a charge transfer between the adsorbed oxygen and the target gas molecules, which leads to a change in surface resistance of the sensor device.<sup>3,6</sup> When a ZnO sensor is exposed to air, an oxygen molecule adsorbs on the surface of the material and forms an O<sub>2</sub><sup>-</sup> ion that creates a high resistance state in air and a high sensitivity.<sup>1</sup> This is the reason ZnO gas-sensor devices have been fabricated as single crystals, thin films, nanorods, and various other nanostructures with small grain sizes. The adsorption reaction may occur due to a very high surface area-to-volume ratio, allowing for higher sensitivity in gas sensing.<sup>1,3,5</sup>

In addition to ZnO nanostructures for higher sensitivity, ZnO is often doped with different materials to create catalytically active sites on the surface of the hydrogen gas sensor. This increases the dissociation of hydrogen to its more reactive form, increasing the selectivity of the gas-sensor device to hydrogen gas.<sup>4,5</sup> Specifically, the selectivity for detecting hydrogen with ZnO nanorods was greatly magnified by the doping of Pd onto the surface of the nanorods.<sup>2</sup> The addition of Pd to ZnO thin films resulted in a reduction of conductance due to an increase in oxygen absorption, which increased the sensitivity from 40% for ZnO to 99.8% in the doped ZnO.<sup>6</sup> One of the main problems with commercial sensors is that they operate at high temperatures, which degrades the material and also decreases the stability and recoverability of these devices. Doping ZnO with Pd has been shown to increase the stability of the nanorod and thin-film sensor devices and has also

improved the response and recovery time of these devices to hydrogen gas.<sup>3</sup> The reason that Pd particles enhance the gas-sensing ability of oxides is that when Pd particles are exposed to hydrogen, they adsorb the gas and swell slightly to form palladium hydride. The different oxide gas sensors rely on the different conductivity of palladium and palladium hydride to indicate hydrogen concentration.<sup>7</sup>

This study was aimed at comparing the doping effects of Pd on ZnO 2-D nanostructure thin-film sensors as well as optimizing the concentration of Pd in order to enhance the performance of these different gas-sensor devices to hydrogen gas in terms of the sensitivity, selectivity, stability, and response and recovery time.

### Approach

In order to study the effect of Pd dopant on ZnO thin-film gas-sensor devices, different sol gels for the silicon substrate were prepared using 0%, 1%, 2%, 4%, and 8% of Pd and 0.9M ZnO. These doped 0.9 M ZnO sol gels were then spin-coated onto silicon oxide substrate three times and annealed at 700° C for 1 hr to create a 2-D thin-film nanostructure. In order to compare the effect of size on the sensitivity of ZnO, 1-D nanolines were fabricated using pure 0.1 M ZnO by soft-electron beam lithography.

SEM images were taken of the annealed samples at 50k, 60k, 80k, and 100k magnification settings in order to determine the effects of the different concentrations of Pd on the grain structure of ZnO thin film. SEM images were also taken of the cross-section of the ZnO thin film to determine the thickness of the film. SEM images were also taken of the 1-D ZnO nanoline. EDS was conducted using the Hitachi 4800 SEM to confirm the presence of Zn, O, and Pd on the ZnO thin-film samples; XPS was used as a more sensitive measure than EDS to determine the presence of these elements; and ICP was used to determine the concentrations of the dopants in the ZnO sol gels. XRD was then used to determine the crystal structure of the annealed ZnO thin films.

For the gas-sensing component of this research, the actual sensor devices were fabricated using photolithography. Pt electrodes were made on top of the ZnO thin film using the photolithography process, and after the electrodes were selected and connected to the chip carriers, the samples were then placed in a measurement chamber with a 40-channel switching system to measure the resistance of the samples, a UV LED, and a flow controller unit to control the gas flow. The NanoNose™ Software Tool was used to collect and analyze the resistance data. The three main gas-sensing assessments of the Pd-doped ZnO thin films were then conducted.

Instead of being heated up to operating temperature, as in commercial sensing, the ZnO 2-D nanostructures were exposed to UV light. UV light causes photo excitation of electrons on the surface of the semiconductor oxide sensor and the formation of electron holes, aiding in the absorption of hydrogen. UV light reduces the need for heating the material up to high operating temperatures and also uses less power input to operate. Measurements were taken of the change in resistance of the thin films with and without UV light in order to determine its effect on the sensitivity measurements of Pd-doped ZnO thin film. For measurements with the UV light, a voltage of 4V was applied with a current of 1.05 A. The resistance of the thin-film device with both UV and non-UV exposure was measured under total air flow of 100 sccm with three cycles of 15 min of 2.5% total hydrogen gas flow and then 30 min of recovery time in order to determine the stability of the thin film.

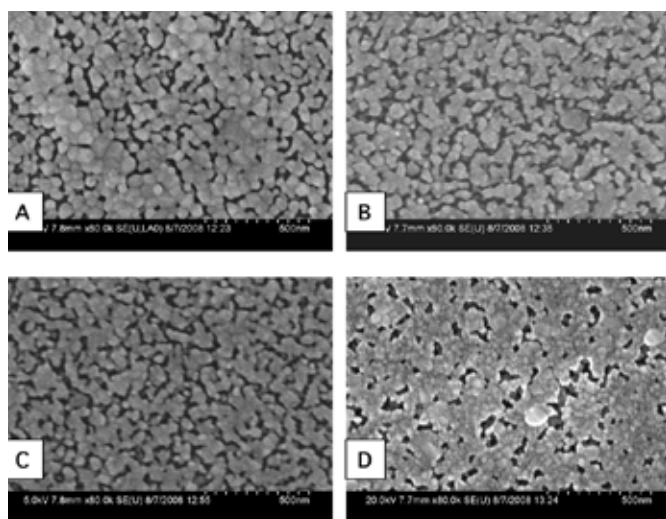


Figure 4. All the SEM images of the annealed Pd-doped ZnO thin-film samples were taken at 80 k magnification. (A) 0%Pd ZnO (B) 1% Pd ZnO (C) 2% Pd ZnO (D) 8% Pd ZnO.

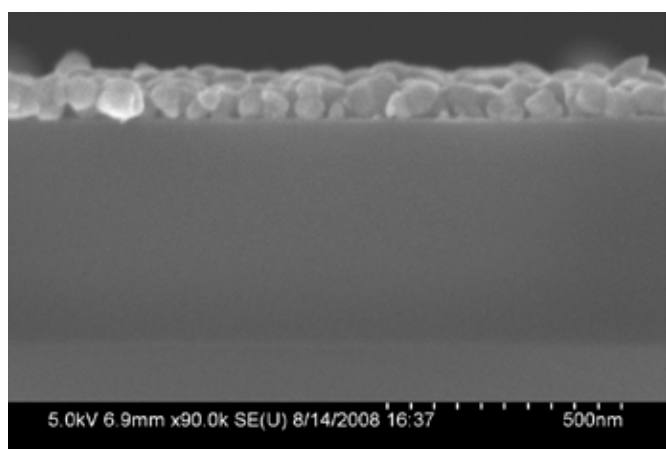


Figure 5. The cross-section of the thin film shows that the thickness of the ZnO thin film is about 90 nm. The SEM image of the ZnO nanoline shows a structure with less porosity and smaller grain sizes than the ZnO thin film.

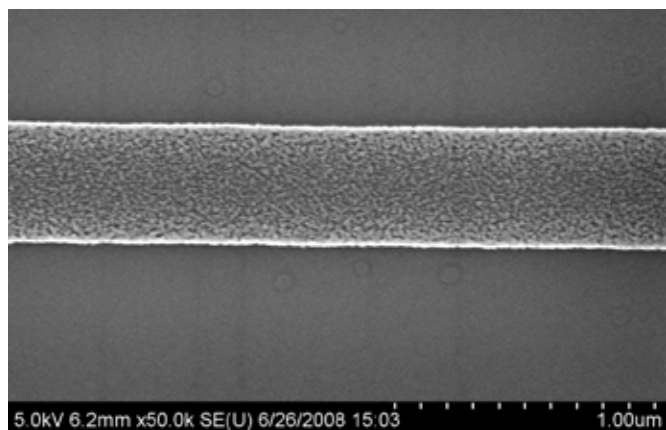


Figure 6. SEM of ZnO nanoline about 400 nm in width.

The second major analysis of the hydrogen-sensing characteristics of ZnO thin film compared the ZnO thin film and the TGS 821 commercial sensor to determine a difference in performance. Both samples were analyzed at room temperature with UV light exposure and three cycles of 100 sccm (2.5%) hydrogen gas flow. Although this research involved mostly the analysis of 2-D ZnO nanostructures, the third analysis involved the same conditions as the previous analysis but compared the 2-D ZnO thin film and the 1-D ZnO nanoline to determine which dimensional structure had a better sensitivity in response to hydrogen gas flow. For all of the analysis involving UV light exposure, the samples were exposed to UV light for 1 hr prior to the three-cycled testing in order to stabilize the sample.

### Results

#### Nanostructure Characterization

After the Pd-doped 0.9 M ZnO thin films were fabricated and annealed, grain-structure characterization of the films was done using SEM imaging. The SEM images revealed that the annealed ZnO thin films were crystalline, with grains between 50 and 100 nm in diameter. The Pd-doped ZnO samples showed slightly decreasing grain size with increasing dopant concentration. All of the ZnO thin films showed a much higher porosity than what was expected.

In order to determine the composition of the annealed grains, EDS was conducted using the SEM. The EDS spectra of the Pd-doped ZnO samples showed that the annealed thin film was made up of ZnO, but, since the film was very thin, the largest peak on the spectrum is for silicon from the silicon substrate. The spectrums showed a very low peak for Zn compared with the peak for silicon. This indicates that the exact concentration of the ZnO thin film was not great enough to be detected by EDS.

In order to determine the exact concentration of Pd that was incorporated into the ZnO sol gels, ICP was done on the Pd-doped sol gels using Pd ICP standards. The results revealed actual concentrations that were close to the theoretical concentrations.

In order to determine the crystal structure of the annealed thin films, XRD was conducted on the Pd-doped ZnO thin films. The resulting XRD spectra were consistent with the ZnO crystal peaks.

#### Gas-Sensing Characterization

After using photolithography to create electrode masks on all the thin-film samples and then sputter-coating the Pt layer and developing it to leave electrodes on top of the thin film, this project used optical microscopy to determine the best electrodes for making the sensor devices.

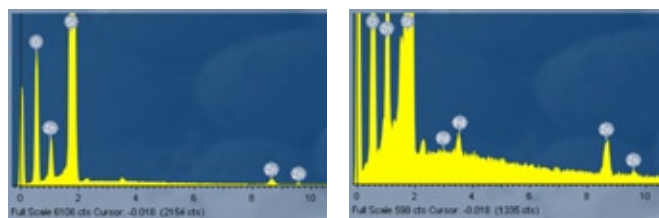
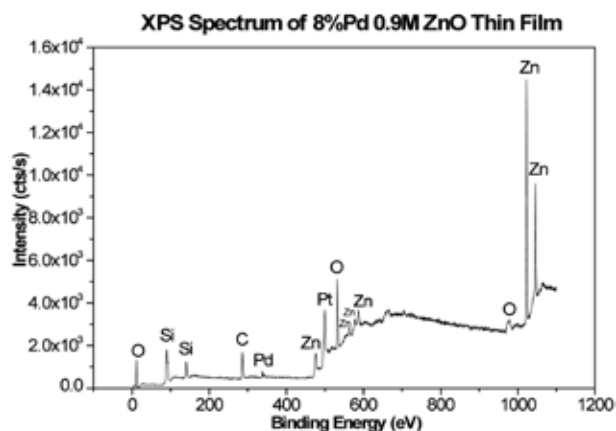
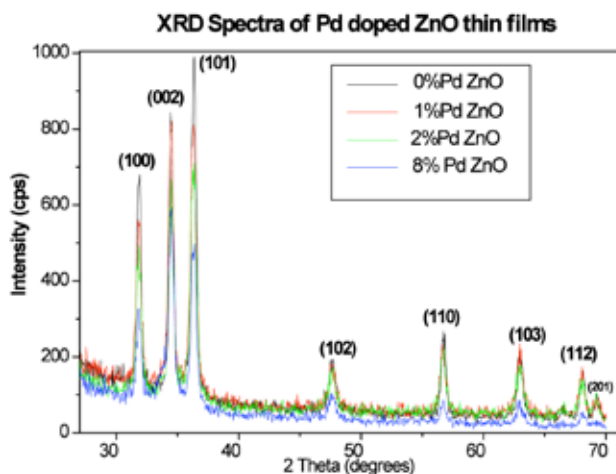


Figure 7. (Left) EDS spectrum of 0% Pd ZnO thin film showing Zn, O, and Si peaks. (Right) EDS spectrum of 1%Pd ZnO thin film showing Zn, O, Si, and Pd peaks. A more sensitive measure of the composition of the annealed thin films was done using XPS, a surface-chemistry analysis technique. The XPS data showed that Pd was present for high concentrations of dopant in the ZnO thin films.



**Figure 8.** XPS Spectrum of 8% Pd ZnO thin film indicating primarily the presence of Zn, O, Pd, and Si.



**Figure 10.** XRD spectra of Pd-doped ZnO annealed thin films showing consistent ZnO crystal peaks for all concentrations of Pd dopant. The strongest peaks for ZnO are (101), (002), and (100).

After the best electrodes were selected, cut, and wire-bound to the chip carriers, the electrical property measurements were finally conducted. However, due to the extremely high porosity (which will be explained in the discussion) of the Pd-doped samples, electrical testing could not be conducted on the Pd-doped ZnO samples. Rather, the three analyses were performed using only the 0% Pd ZnO samples.

The first analysis was the 0% Pd ZnO thin-film gas sensing of hydrogen with and without exposure to UV light conducted at room temperature. The results without UV light show that there was roughly no change in resistance with the application of hydrogen gas flow; rather than going down, the resistance increased over the course of the three cycles of gas flow and recovery. The results with the UV light showed that with each exposure to hydrogen gas, the resistance of the ZnO thin film went down. The sensitivity of the ZnO thin-film sensor can be measured by the change in the resistance due to change in the concentration of applied gas. The sensitivity for each application of hydrogen flow was around 12%.

Percent Pd	Measured Percent Pd
1%	0.99%
2%	1.99%
4%	3.88%
8%	8.87%

**Figure 9.** ICP data for different concentrations of Pd-doped ZnO sol gels, showing the difference between the theoretical concentration and the measured concentration of Pd in the sample.



**Figure 11.** Pt electrodes sputtered on top of ZnO thin film, showing a clean shape and gap of about 10  $\mu\text{m}$  between electrode pairs.

The second analysis conducted compared the pure 0.9 M ZnO thin-film sensor and the TGS 821 commercial sensor. The measurements were taken with UV light exposure at room temperature with three cycles of 100 sccm (2.5% total) hydrogen gas flow.

The second analysis included a comparison in the change of sensitivity with each exposure to hydrogen and the change in the baseline resistance with each exposure to hydrogen. These are measures of the response and recovery of the sensors; the greater the drift, the more quickly the sensor will degrade. The commercial sensor has a higher drift rate than the thin-film sensor; this is also true with the baseline drift rate.

Because there was such difficulty in measuring the resistance of the Pd-doped ZnO thin-film samples due to high porosity, analysis was conducted comparing the sensitivity of the 2-D ZnO thin-film nanostructure and the 1-D ZnO soft-electron-beam-patterned ZnO-400 nm-wide nanoline. The results revealed a higher sensitivity for the 1-D ZnO nanoline (about 19%) than for the thin film (12%).

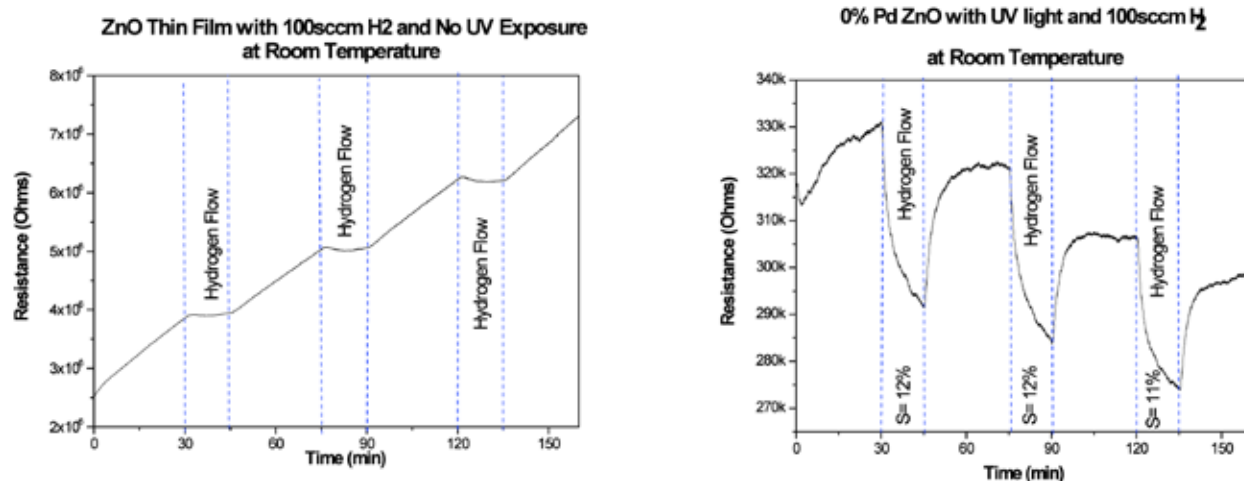


Figure 12. (Left) Resistance results for 0% Pd ZnO thin film with UV light exposure at room temperature conducted with three cycles of 100 sccm (2.5%) hydrogen gas flow. (Right) Resistance results for 0% Pd ZnO thin film with no UV light exposure.

**Discussion**

*Nanostructure Characterization*

The SEM images of Pd-doped ZnO showed slightly decreasing grain sizes with increasing dopant concentration. A comparison of these results with the literature about dopant effect on grain structure shows that increasing dopant concentration should result in smaller grains, which was the effect observed in this research. However, there was high porosity in all the Pd-doped ZnO thin-film samples regardless of Pd concentration. The grains must be quite close together for the conductivity and proper resistance to be measured. The porosity must be optimized so that there is enough for absorption but not so much as to hinder the electrical resistance measurements. However, because the porosity was so high and the grains could not come into close contact, the resulting resistance measurements of the Pd-doped samples were very high. Due to the high porosity and poor resistance measurements, full analysis could not be conducted with the Pd-doped ZnO thin-film samples. However, the ZnO nanoline showed grain shrinkage with annealing and less porosity than the ZnO thin films.

The composition of the ZnO-annealed thin films was determined using EDS, and XPS was used to determine the various elements in the thin film rather than to determine the specific concentrations of these elements in the films. A problem with the EDS analysis was that the samples had very thin layers of film, allowing the electron beam to penetrate into the silicon region of the substrate and causing a much higher peak of silicon to occur in the EDS than for the peaks of the actual elements in the annealed thin films themselves. This led to inaccurate concentration results. In order to accurately determine the concentrations of the different elements in the ZnO annealed thin-film samples, tunneling electron microscopy (TEM) can be used to cross-section samples and determine the composition of the annealed thin films.

The XRD spectra confirmed a crystal structure consistent with ZnO for all concentrations of Pd with no presence of second phases or shifts in d-spacing.

*Gas-Sensing Characteristics*

The first analysis of ZnO thin-film hydrogen gas sensing showed a huge improvement in sensitivity with the application of UV light. This is a good indication that UV light can be used to improve the sensitivity of the ZnO thin-film gas sensor without raising the temperature of the material and while using less power.

The second analysis comparing the commercial sensor with the ZnO thin-film sensor shows that although the commercial sensor had a higher sensitivity, the drift rates were much higher than those for the ZnO sensor. These results show that ZnO sensors are more stable and have a higher recovery than the commercial sensors at room temperature with the exposure of UV light.

The third analysis was done primarily to determine the effect of size on the sensitivity of ZnO. The 1-D ZnO nanoline showed a much higher sensitivity than the 2-D thin film. This is because the 2-D thin film was highly porous, and the 1-D nanoline experienced grain shrinkage due to annealing. Because of the improvement in sensitivity

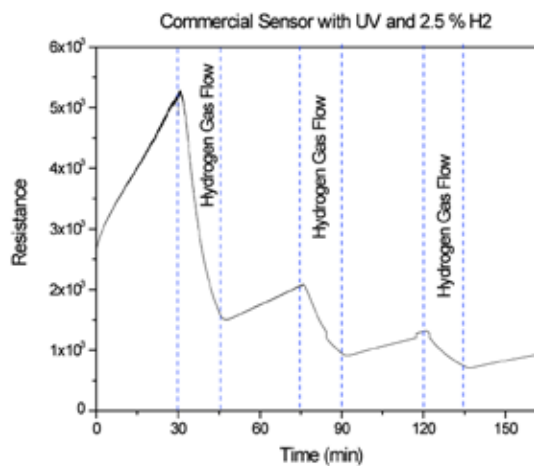
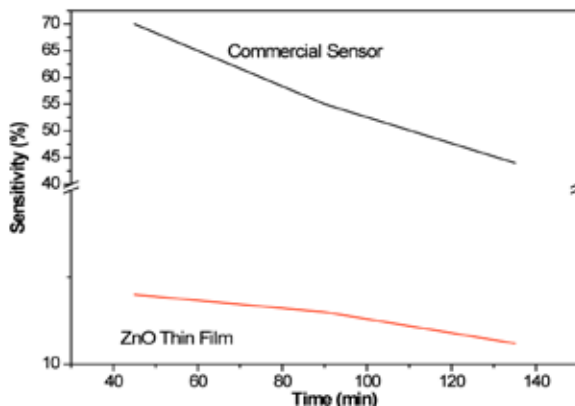
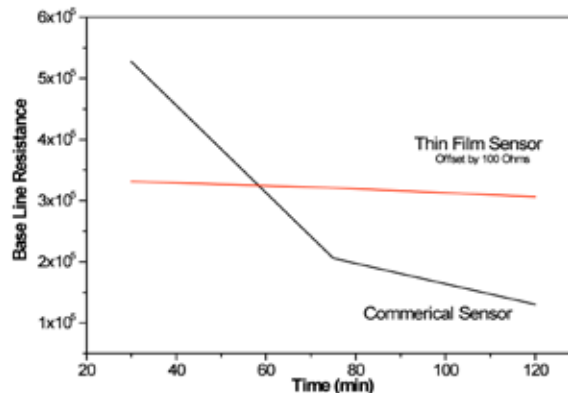


Figure 13. Previous data collected of TGS 821 commercial sensor with UV light exposure and three cycles of 2.5% total hydrogen.

**Sensitivity Drift for Commercial and Thin Film Sensor at Room Temperature**



**Base Line Drift For Commercial and ZnO Thin Film Sensor at Room Temperature**



**Figure 14.** (A) The sensitivity drift rate shows a steeper drift for the commercial sensor than for the ZnO thin-film sensor. (B) The baseline drift rate shows a steeper drift for the commercial sensor than for the ZnO thin-film sensor.

from the transition from 2-D nanostructures to 1-D nanostructures, the primary focus of future study will move from 2-D nanostructure sensor devices to 1-D nanostructure sensor devices.

### Conclusion

Different concentrations of Pd-doped ZnO sol-gels were used to fabricate 2-D nanostructures; they proved to be a simple, versatile, and inexpensive method of making sensor devices. One of the most important observations coming from the nanostructure characterization was that there was extremely high porosity in Pd-doped ZnO 2-D nanostructures, resulting in poor resistance measurements. EDS, XPS, and ICP confirmed the presence and concentration of Pd in the ZnO thin-film samples and sol gels, and the XRD results confirmed a crystal structure consistent with ZnO for all concentrations of Pd, with no presence of second phases or shifts in d-spacing. For the gas-sensing characterization, UV light exposure increased the sensitivity of ZnO in response to hydrogen, and the ZnO thin film showed a better recovery than the commercial sensor at room temperature. The most important conclusion reached from the results of the gas-sensing measurements of the 2-D thin film compared with the 1-D nanoline is that smaller grain sizes (larger surface area), with a transition from 2-D nanostructure to 1-D nanostructures, increases the sensitivity of ZnO sensor devices in response to hydrogen gas.

There are several implications for the future. The next step involves using different Pd-doped ZnO sol gels to fabricate smaller nanopatterned structures such as nanolines by soft-electron beam lithography for a greater surface-to-volume interaction than thin films. To continue testing on the 2-D nanostructures necessitates optimizing the annealing

**ZnO 400nm Nanoline with UV light and H<sub>2</sub> at Room Temperature**

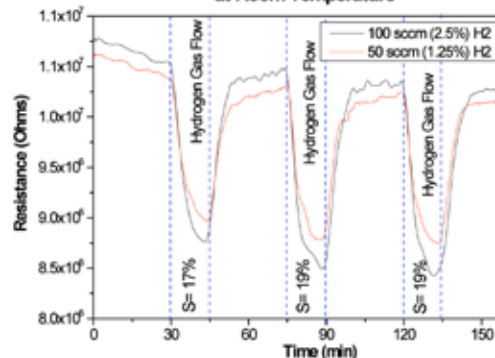


**Figure 15.** Gas-sensing results of 0.1 M ZnO 400 nm nanoline with UV light exposure at room temperature with three cycles of 2.5% total hydrogen flow.

temperature and annealing time to refine the grain sizes and reduce the porosity of the thin films. Other possibilities include using other dopants and testing of other gases.

*This research was supported primarily by the Northwestern University Nanoscale Science and Engineering Research Experience for Undergraduates (REU) program under NSF award number EEC-0755375. Any opinions, findings, and conclusions or recommendations expressed in this material are those of the author(s) and do not necessarily reflect those of the National Science Foundation.*

### References

- Wang et al. *Appl. Phys. Lett.* **2004**, *84*, 18, 3654–3656.
- Wang et al. *Appl. Phys. Lett.* **2005**, *86*, 243503–(1–3).
- Mitra, P.; Chatterjee, A. P.; Maiti, H. S. *Materials Letters* **1996**, *35*, 33–38.
- Tien et al. *Appl. Phys. Lett.* **2005**, *87*, 222106–(1–3).
- Franke, M. E.; Koplin, T. J.; Simon, U. *Small* **2006**, *2*, 1, 36–50.
- Yamazoe, N.; Shimanoe, K.; Sawada, C. *Thin Solid Films* **2007**, *515*, 8302–8309.
- Donthu, S.; Sun, T.; Dravid, V. *Adv. Mater.* **2007**, *19*, 125–128.